# ELECTRIC FIELD INDUCED INTERFACIAL INSTABILITIES

Robert E. Kusner[1], Kyung Yang Min[2], [1,2]NASA Lewis Research Center, [1]rkusner@lerc.nasa.gov, [2]kym0270@lerc.nasa.gov, Xiao-lun Wu[3], [3]University of Pittsburgh, wu@vms.cis.pitt.edu, Akira Onuki[4], [4]Kyoto University, Kyoto, Japan

## 1 INTRODUCTION

Several systems exhibit an interfacial instability in response to a stress resulting from the application of an external field. Two such systems closely related to the proposed system of study are a ferrofluid/air interface in the presence of a magnetic field [1, 2], and the interface between two fluids when charged with ions [3, 4, 5, 6]. Both systems lead to the formation of a hexagonal dimple pattern. One of our collaborators, Prof. A. Onuki, has recently proposed that such an effect could be observed at the neutral two-phase interface of a critical system, such as a binary fluid near its consolute point, or a simple fluid near the critical point of its liquid/vapor transition, in the presence of an externally applied electric field [7].

An undulation instability of interfaces between two immiscible dielectric fluids was studied using an oscillating electric field. The binary system studied was a mixture of aniline and cyclohexane (AC). The aniline component is slightly polar, making the aniline rich phase significantly more conductiong than the cyclohexane rich phase. The critical electric field $E_c$, at the onset of instability, was measured as the frequency was varied at several different temperatures.

At lower frequencies, column-like structures were formed. When the critical field was plotted as a function of reduced temperature $\epsilon$, it exhibited a power-law relationship, $E_c \sim \epsilon^{\zeta}$, where $\zeta \sim 0.34$. This compares well with the value $\zeta \sim 0.4$ for a system of conducting and non-conducting fluids.

At higher frequencies, the charge carriers in the conducting fluid can do not respond quick enough; the electric fields in the system are determined by its dielectric properies. In such a case, the interface becomes unstable due to the difference in the dielectric constants of the two phases. Measurement at a high frequency limit displayed two major differences from that of a lower frequency limit. First, localized elevation of interfacial surface was observed as opposed to column-like protusions, and secondly, $E_c \sim \epsilon^{\zeta}$, where $\zeta \sim 0.08$. The measured value of $\zeta$ is in good agreement with the theoretically predicted value $\zeta = 0.07$.

## 2 EFFECT OF ELECTRIC FIELD ON THE INTERFACE

The change in the free energy due to a capillary surface wave with wave number $k$ is proportional to

$$G_k = \sigma k^2 - C_E k + g(\Delta\rho) \quad (1)$$

$$= \sigma(k - \frac{C_E}{2\sigma})^2 - \frac{C_E^2 - 4\sigma(\Delta\rho)g}{4\sigma}, \quad (2)$$

where $\sigma$ is the surface tension, $g$ is the gravitational acceleration, and $\Delta\rho$ is the mass density difference between the two phases, taken to be positive. The parameter $C_E$ represents the effect of electric field on the binary system. For a cell filled with a critical binary mixture where the interface is formed at the middle of two electrodes near the critical temperature, $C_E$ is represented by

$$C_E = \frac{1}{\pi}\frac{\varepsilon_1\varepsilon_2(\varepsilon_2 - \varepsilon_1)^2}{(\varepsilon_1 + \varepsilon_2)^3}(\frac{V}{d})^2. \quad (3)$$

Here $d$ is the separation of electrodes, $V$ is the applied voltage, and $\varepsilon_1$ and $\varepsilon_2$ are dielectric constants of two phases, respectively. The first and third term in Eq. (1) are the standard expressions used to describe a capillary wave on a liquid surface. The second term is the effect of the electric field and the source of the instability. Equation (2) shows that $G_k$ takes a minimum at wave number $k^* = C_E/2\sigma$ and that the surface fluctuation at $k = k^*$ becomes unstable for $C_E^2 > 4\sigma(\Delta\rho)g$. This condition, together with eq. (3), determines the critical ( or threshold) electric field $E_c$:

$$E_c = \frac{1}{\varepsilon_2 - \varepsilon_1}\sqrt{\frac{2\pi(\varepsilon_1 + \varepsilon_2)^3}{\varepsilon_1\varepsilon_2}}\sqrt[4]{\sigma(\Delta\rho)g}. \quad (4)$$

Upper and lower boundaries of Eq. (4) based on $\varepsilon_2/\varepsilon_1 \to \infty$ or $\varepsilon_2/\varepsilon_1 \sim 1$ represent the conducting and non-conducting limits, respectively. In this calculation, two well-known relationships were used: $\sigma \cong \sigma_0\epsilon^{2\nu}$[8, 9] and $\varepsilon_2 - \varepsilon_1 \cong \varepsilon_0\epsilon^{\beta}$ with $\nu = 0.625$ and $\beta = 1/3$[10].

1. Conducting limit ($\varepsilon_2/\varepsilon_1 \to \infty$):

$$E_c \sim \sqrt{\frac{2\pi}{\varepsilon_1}}\sqrt[4]{\sigma(\Delta\rho)g} \sim (\epsilon^{2\nu}\epsilon^{1/3})^{1/4} \sim \epsilon^{0.4}. \quad (5)$$

G. I. Taylor used alternate derivation of the first form in Eq. (4) and it was verified experimentally in a few systems (water-air, water-oil, mercury-air, and mercury-oil)[11].

2. Non-conducting limit ($\varepsilon_2/\varepsilon_1 \sim 1$):

$$E_c \sim \epsilon^{-1/3}(\epsilon^{2\nu}\epsilon^{1/3})^{1/4} \sim \epsilon^{0.07}. \qquad (6)$$

Later when figure 3 is discussed, more precise definition of the non-conducting limit will be presented.

In the case of an alternating electric field $E = E_0\cos(\omega t)$, the frequency $\omega$ influences current flow in a material with an ohmic conductivity $\kappa$ in addition to its dielectric properties (dielectric const $\varepsilon$). In such a leaky dielectric, the polarization current is $\vec{j} = \partial(\varepsilon\vec{E})/\partial t \sim \omega\varepsilon\vec{E}$ and the current density due to the migration of free charge is $\vec{j} = \kappa\vec{E}$. The ratio of these two currents, $\omega\varepsilon/\kappa$, decides whether the system behaves as a conducting or non-conducting system[12]. At low frequency limit ($\omega \ll \kappa/\varepsilon$), the interface charge is that for a static interface and the system behaves as a conductor. At high frequency limit ($\omega \gg \kappa/\epsilon$), conducting processes should be inhibited and the free charges remain neutralized, leaving only a residual polarization charge at the interface. Therefore, the temperature dependence of the threshold electric field in the aniline and cyclohexane (AC) system will be manifested as follows:

1. When $\omega \ll \kappa/\varepsilon$, $E_c \sim \epsilon^{0.4}$.
2. When $\omega \gg \kappa/\varepsilon$, $E_c \sim \epsilon^{0.07}$.

## 3 EXPERIMENTAL

The sample cell was constructed of two indium/tin oxide (ITO) coated electrodes cemented to a glass spacer of rectangular shape. The separation between electrodes was 4mm. The cell was immersed in an oil bath (Dow Corning 200 fluid, viscosity=1.5 cSt), whose temperature was controlled by a surrounding water bath. The temperature of the oil bath was kept constant with a precision of ± 0.5 mK/day. For the AC binary system, the critical concentration of aniline was 0.444 mole fraction and the critical temperature was $T_c = 32.70°$C. Dielectric constants of pure cyclohexane and aniline are 2.03 and 6.86, respectively[13].

The AC system was found to be light-sensitive with its critical temperature drifting with time. Such a drift of temperature was offset by re-measuring $T_c$ for each set of measurements. All the temperature scales described below were calibrated in this way. Due to the degradation of the sample, only four sets of measurements will be presented.

Figure 1: Instability observed at $\Delta T = 120$mK and $f = 200$Hz. The upper phase is cyclohexane-rich and the bottom aniline-rich. As the frequency increases, the pattern of strings changed from finer to coarser one.

An ac-amplifier (Trek, Inc. Model 609D-6) with a 4 kV peak ac output and a small signal bandwidth of 35 kHz was used to generate an oscillating field perpendicular to the interface. In order to observe interfacial instability, the temperature $T$ was lowered below $T_c$ to the desired value and frequency was set to $f = \omega/2\pi = 10$Hz. The amplitude of the field was raised gradually until instability was seen. Near the onset, even a small change of the voltage amplitude generated the instability, thus enabling the critical field $E_c$ to be measured with an accuracy of 2%. The rms value of the critical voltage was recorded by a multimeter (Keithley, Model 2001). Next frequency was increased stepwise and the whole process was repeated for a few different temperatures.

At a lower frequency ($f \sim 10$ to $f \sim 1000$Hz), many string-like structures were formed in the cyclohexane-rich phase. This observation is very similar to what was seen in G. I. Taylor's experiment[11, 14]. There the interfacial agitation and occasional isolated points rose from the conducting to non-conducting fluid as the critical voltage for instability was approached. The string spanned the space between the interface and one of the electrodes, and had a life time of several seconds. When the field was abruptly turned off, each string split into a few pieces, all of which eventually fell to the interface in a couple of seconds.

Figure 1 shows such a structure formed at $\Delta T = 120$mK and $f = 200$Hz. Due to a bubble near the filling tube which is at the left top of figure, the field was not uniform across the cell, resulting in a localized

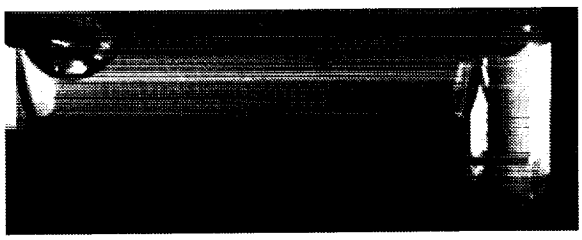

Figure 2: Instability observed at $\Delta T = 120$mK and $f = 3500$Hz. The localized convective motion of the upper fluid seen in Fig. 1 is absent for this relatively high frequency.

convective motion of the upper fluid in the left side of the cell. Nonetheless the pattern formed on the right half of the cell was almost stationary.

At a higher frequency ($f \sim 1000$ to $f \sim 13,000$Hz), many locally elevated areas (of cone shape) were formed as shown in Fig. 2. At such a high frequency, when the applied field exceeded the critical value by a small amount, a rigorous mixing of the two phases across the interface was observed.

When $E_c$ was plotted as a function of frequency for a fixed temperature, the plot was of the sigmoidal shape with two flat regions in a low and high frequency limit, respectively. Figure 3 shows measurements for two different temperatures, $T = 31.12$°C and $T = 32.56$°C. Two additional measurements obtained at $T = 31.89$°C and $T = 32.44$°C are not shown in this figure. However, they exhibit the same shape and fall in between the two curves represented.

It is interesting to note that the sigmoidal shape observed here can be obtained by replacing $\varepsilon_j$ with $|\varepsilon_j + 4\pi\kappa_j \cdot i/\omega|$ ($j$ =1, 2 and $i = \sqrt{-1}$) in Eq.(4)[15]. In this theoretical approach, the non-conducting limit, $\kappa_j \to 0$ for $j = 1, 2$, is obtained by taking a limit: $4\pi\kappa_j/\omega \ll \epsilon_j$ for $j = 1, 2$ or simply $\omega \to \infty$. Obviously, such a non-conducting limit should correspond to the plateau of each curve in Fig. 3. In order to fit the curves in this figure, the magnitude and phase lag of the current should be measured as a function of frequency for this leaky dielectric[12]. However, this was not possible because of the fast degradation of the sample.

Figure 4 is a log-log plot of critical electric field $E_c$ vs. reduced temperature $\epsilon$ for five different frequencies. It was obtained from Fig. 3 by reading $E_c$ as a function of $T$ for a fixed frequency (the measurements at $f = 0$ is not shown in Fig. 3). Note that the slope in this figure yields the critical exponent $\zeta$ in the relation $E_c = \epsilon^{\zeta}$.

The dependence of the critical exponent $\zeta$ on fre-

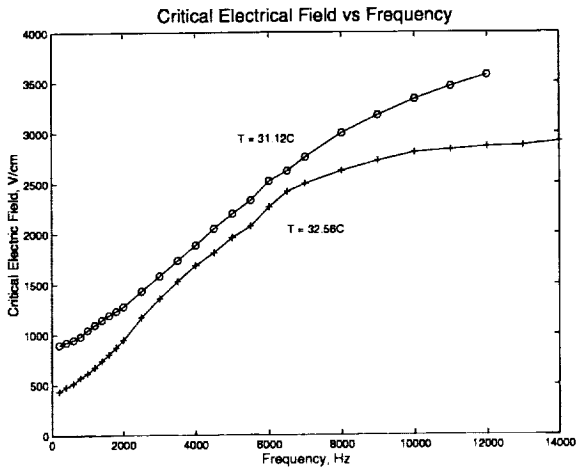


Figure 3: Plot of critical electric field vs frequency. The curve marked with '+' sign levels off for high frequencies ($f \geq 10000$Hz). In the measurement corresponding to the curve marked with '0' sign in the same figure, the critical electric fields above $f$ =12000Hz could not be obtained, due to the instrumental limitation of the amplifier used.

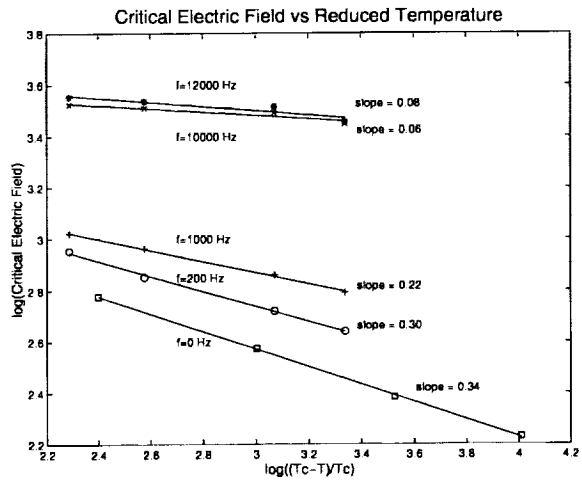


Figure 4: Log-log plot of critical electric field as a function of reduced temperature for fixed frequencies. Solid lines are linear regression fit to data.

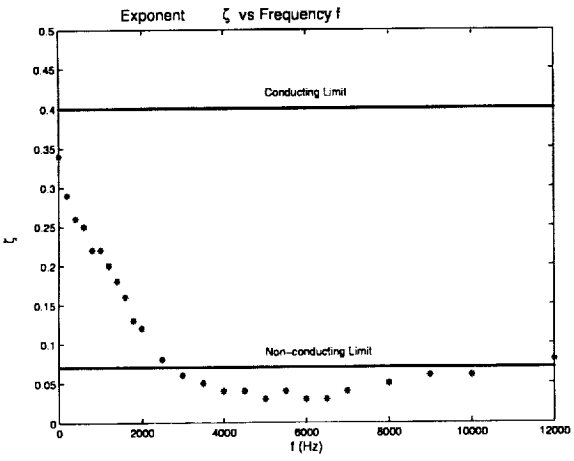


Figure 5: Critical exponent $\zeta$ vs frequency f. Two horizontal lines are the conducting and non-conducting limits, respectively. For $f \geq 2500$Hz, the critical exponent is close to the value of the non-conducting limit.

quency $f$ is plotted in Fig. 5. The range of the frequency representing the plateau of the curves in Fig. 3 do not coincide with the range, $f \geq 2500$Hz, where the critical exponent $\zeta$ levels off in Fig. 5. This implies that the approach to the value $\zeta = 0.07$ is not a sufficient condition for the system to behave as a non-conducting medium.

# 4 CONCLUSION

Measurements with a time-varying electric field seems to produce substantially more instructive information about the instability than static-field measurements. With a judicious choice of a sample such as a marginally polar AC system, and by varying the frequency of the applied field, both the conducting and non-conducting limits of an interfacial instabilities could be probed in a systematic fashion. Two control parameters, temperature and frequency, allow us to effectively change the surface tension, the dielectric constant and the ohmic conductivity of each phase. Currently we are investigating similar effects with an alternate binary system, methylene iodide/cyclohexane. The dielectric constant for the methylene iodide is similar to that of aniline but without the toxicity. However certain precautions are being taken, since methylene iodide is also light-sensitive. We are building a new cell, where a copper layer on the electrode will stabilize the light-sensitive nature of methylene iodide.

# 5 ACKNOWLEDGEMENTS

Support to study the effect of electric field instabilities in a two phase fluid interface has been provided to General Vacuum, Inc. by the National Aeronautics and Space Administration under contract # NAS3-2789.

## References

[1] M. D. Cowley and R. E. Rosensweig, J. Fluid Mech. **30**, 671 (1967).

[2] A. Gailitis, J. Fluid Mech. **82**, 401 (1977).

[3] L. P. Gorkov and D. M. Chernikova, Pis'ma Zh. Eksp. Teor. Fiz. **18**, 119 (1973) [JETP Lett. **18**, 68 (1973)].

[4] K. Mima, H. Ikezi and A. Hasegawa, Phys. Rev. **B14**, 3953 (1976).

[5] A .P. Volodin, M. S. Khaikin and V. S.Edel'man, Pis'ma Zh. Eksp. Teor. Fiz. **26**, 707 (1977) [JEPT lett. **26**, 543,(1977)].

[6] M. Wanner and P. Leiderer, Phys. Rev. Lett. **42**, 315 (1979).

[7] A. Onuki, Physica A **217**, 38 (1995).

[8] M. Moldover, Phys. Rev. A **31**, 1022 (1985).

[9] E. S. Wu and W. W. Webb, Phys. Rev. A **8**, 2077 (1973).

[10] D. T. Jacobs, J. Phys. Chem. **86**, 1995-1998 (1982).

[11] G. I. Taylor and A. D. McEwan, J. Fluid Mech. **22**, 1 (1965).

[12] W. B. Russel, D. A. Saville, and W. R. Schowalter, Colloidal Dispersions, Cambridge University Press (1989).

[13] D. Beaglehole, J. Chem. Phys. **74**, 5251 (1981).

[14] J. R. Melcher, Phys. Fluids **4**, 1348 (1961).

[15] L. D. Landau and E. M. Lifshitz, Electrodynamics of Continuous Media, vol. 8, Pergamon Press (1984).